Tensile fracture of surface-damaged composite laminates

DUK-HYUN CHOI, WOON-BONG HWANG
Mechanical Engineering, Pohang University of Science and Technology, Pohang 790-784, Korea
E-mail: whwang@postech.ac.kr

Composites are increasingly used in making structures strong and safe and for other purposes. Most composite laminates face damage from the environment since they are mostly located in the outer parts of structures. The strength of the structure is then degraded by stress concentration, dilamination or crack propagation, and so on. Strength degradation of laminates with holes or notches can be predicted by the point stress criterion or the average stress criterion of Whitney and Nuismer [1–3]. However, the fracture strength for locally surface-damaged laminates has not yet been predicted theoretically.

Tsai and Wu [4] gave a strength criterion in terms of the scalar function for anisotropic materials. However, most laminates are symmetric, so that the equation for the fracture strength can be simplified by using the *classical lamination theory*. In this study, therefore, the equation for symmetric laminates is induced and verified by comparison with Lagace's experimental results and Tsai's prediction [5, 6]. Moreover, this equation is modified to predict the fracture strength for the surface-damaged laminates. To verify this modified equation, flawed specimens were fabricated, and the experimental results were compared with those from the equation.

Fig. 1 is the load–strain curve for a uniaxially loaded laminate, showing multiple ply failures leading up to ultimate laminate failure. The total forces and moments at the kth knee in the curve are given by Equations 1–3 where $N^{(n)}$, $M^{(n)}$, $\varepsilon^{0(n)}$, and $\kappa^{(n)}$ are the load, moment, strain, and curvature at the nth section and $[A^{(n)}]$, $[B^{(n)}]$, and $[D^{(n)}]$ denote the modified stiffness matrix [2].

$$\begin{Bmatrix} N \\ M \end{Bmatrix}_{\text{total}} = \sum_{n=1}^{k} \begin{Bmatrix} N^{(n)} \\ M^{(n)} \end{Bmatrix} \tag{1}$$

$$\begin{Bmatrix} \varepsilon^{0} \\ \kappa \end{Bmatrix}_{\text{total}} = \sum_{n=1}^{k} \begin{Bmatrix} \varepsilon^{0(n)} \\ \kappa^{(n)} \end{Bmatrix} \tag{2}$$

$$\begin{Bmatrix} N^{(n)} \\ M^{(n)} \end{Bmatrix} = \begin{bmatrix} A^{(n)} & B^{(n)} \\ B^{(n)} & D^{(n)} \end{bmatrix} \begin{Bmatrix} \varepsilon^{0(n)} \\ \kappa^{(n)} \end{Bmatrix}. \tag{3}$$

In Equation 3, if the laminate is symmetric, all elements of $[B^{(n)}]$, A_{16}, and A_{26} become zero, and the total force is then given by Equation 4 [2].

$$\{N\} = [A]\{\varepsilon\}. \tag{4}$$

The fracture strength is the maximum force divided by the cross-sectional area of the laminate.

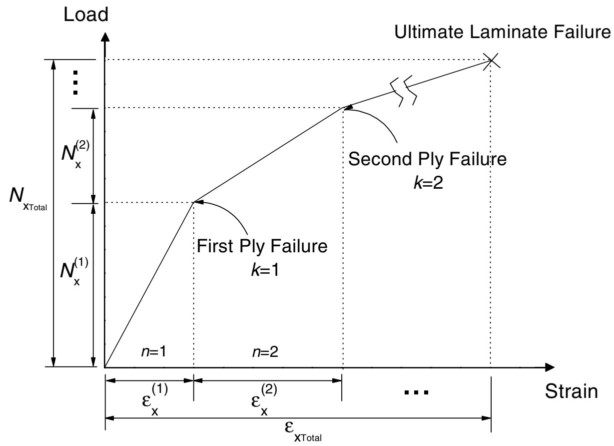

Figure 1 Load–strain curve for uniaxially loaded laminate.

Fig. 2 shows load–strain curves of laminates for four failure models. The main difference is that in the "*G*" path (in the gradual failure model) the straight line is drawn through the initial failure point, whereas in the other paths complete stress relaxation is assumed. The actual path will also depend on the type of loading. If the load is controlled then path "*L*" will be traversed, but a displacement-controlled test will trace path "*D*." An intermediate path "*C*" may also be followed [3]. Tsai and Hahn [6] showed that the "*G*" path is compatible with gradual failure of 90° layers.

Consider now a symmetric laminate subjected to tensile uniaxial loading along the x direction. The laminate consists of plies with n orientations. The classical lamination theory relates the loads and the strains according

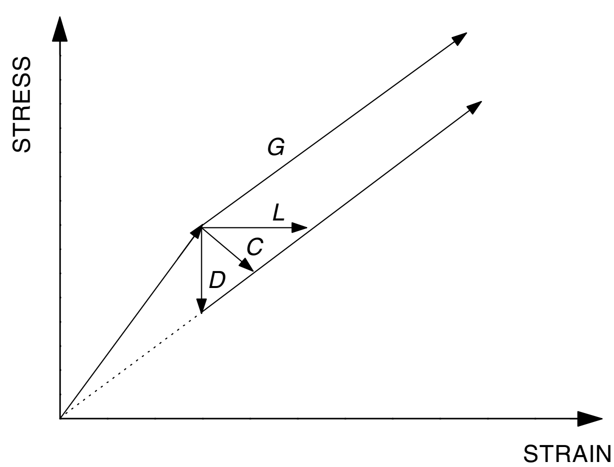

Figure 2 Failure models: *G*—gradual failure; *L, C, D*—complete failure.

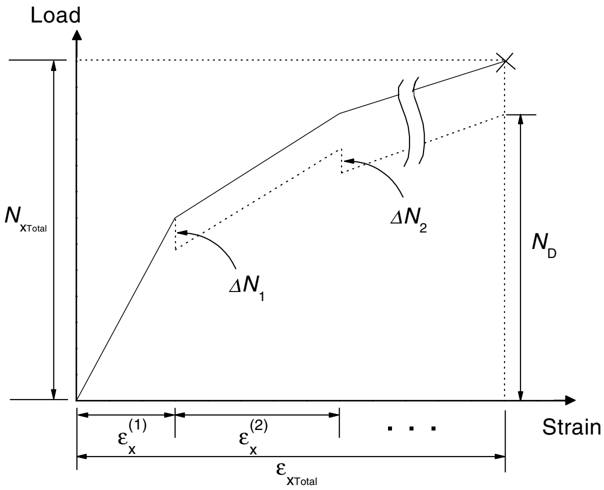

Figure 3 Load–strain curves for symmetric angle-ply laminate under uniaxially loaded. The decrements indicate the relaxed loads.

to Equations 5 and 6.

$$\begin{Bmatrix} N_x \\ 0 \\ 0 \end{Bmatrix} = \begin{bmatrix} A_{11} & A_{12} & 0 \\ A_{12} & A_{22} & 0 \\ 0 & 0 & A_{16} \end{bmatrix} \begin{Bmatrix} \varepsilon_x \\ \varepsilon_y \\ \gamma_{xy} \end{Bmatrix} \tag{5}$$

$$N_x = \left(A_{11} - \frac{A_{12}^2}{A_{22}} \right) \varepsilon_x = K \cdot \varepsilon_x$$

$$\text{where} \quad K = A_{11} - \frac{A_{12}^2}{A_{22}}. \tag{6}$$

If it is assumed that the gradual failure model can be applied to any angle-ply laminates, then in Fig. 3 the load–strain curves for a symmetric angle-ply laminate are given by the solid line in the gradual failure model and by the dotted line in the displacement-controlled test. The slope of each section indicates the corresponding stiffness K, in Equation 6, and the curve has the total $n - 1$ sections until all plies have failed. Equation 7 then represents the total loads, $N_{x\,\text{total}}$, at failure in the gradual failure model, which is the sum of the total load, N_D, in displacement control and the total relaxed load, N_R, given by Equation 8.

$$\begin{aligned} N_{x\,\text{total}} &= \sum_{k=1}^{n-1} \Delta N_k + N_D = N_R + N_D \\ &= \sum_{k=1}^{n-1} \left(K^{(k)} - K^{(k+1)}\right)\varepsilon_k + K^{(n)}\varepsilon_n \end{aligned} \tag{7}$$

$$\begin{aligned} \Delta N_1 &= K^{(1)}\varepsilon_1 - K^{(2)}\varepsilon_1 = \left(K^{(1)} - K^{(2)}\right)\varepsilon_1 \\ \Delta N_2 &= K^{(2)}\varepsilon_2 - K^{(3)}\varepsilon_2 = \left(K^{(2)} - K^{(3)}\right)\varepsilon_2 \\ &\vdots \\ \therefore N_R &= \sum_{k=1}^{n-1} \Delta N_k = \sum_{k=1}^{n-1} \left(K^{(k)} - K^{(k+1)}\right)\varepsilon_k. \end{aligned} \tag{8}$$

Finally, if both the width of the laminate and the thickness of each layer are 1, the thickness of the laminate is the total number of layer, T_{total}, and then the cross-section area of the laminate is also T_{total}. The equation for the fracture strength of symmetric laminate is then given by Equation 9 where T_p is the number of layers broken at the pth sequence. Moreover, in Equation 9, the sequence of strains must be fixed. The fracture strain of ε_i must be less than that of ε_j $(i < j)$.

$$S_{x\,\text{total}} = \frac{1}{T_{\text{total}}} \left[\sum_{k=1}^{n-1} \left(K^{(k)} - K^{(k+1)}\right) e_k + K^{(n)} e_n \right],$$

$$\text{where} \quad K^{(k)} = A_{11}^{(k)} - \frac{A_{12}^{(k)^2}}{A_{22}^{(k)}}, \quad [A]^{(k)} = \sum_{p=k}^{n} T_p [Q]_p. \tag{9}$$

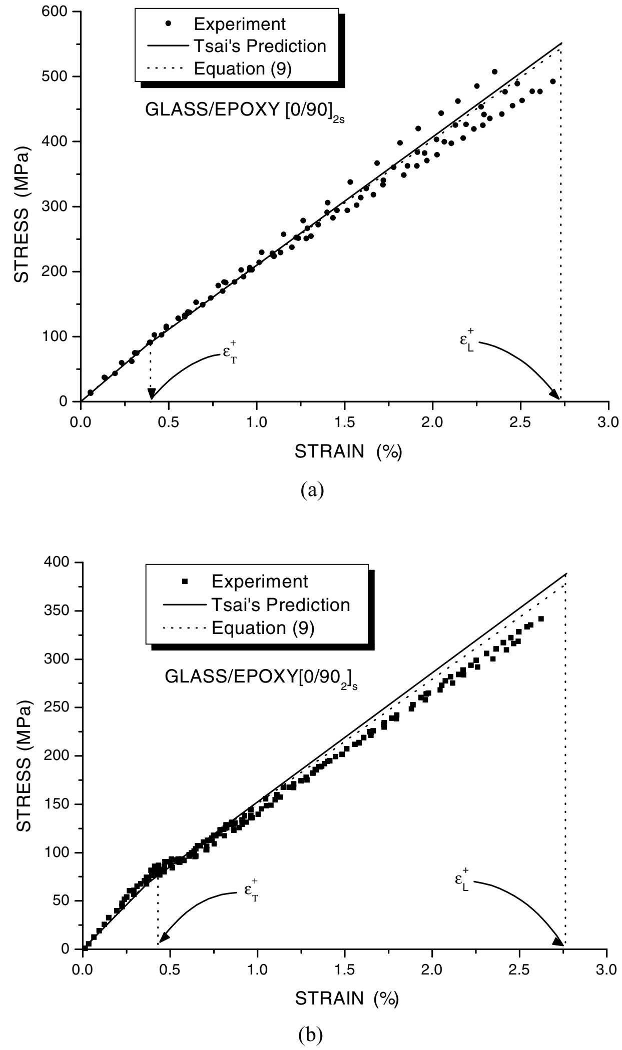

Figure 4 Stress–strain relation of (a) $[0/90]_{2s}$ and (b) $[0/90_2]_s$ glass/epoxy laminate.

To verify Equation 9, its predictions were compared with Lagace's and Tsai's experimental results. Fig. 4 is the graph in which the predictions of Equation 9 were compared with Tsai's experimental results and his predictions for $[0/90]_{2s}$ and $[0/90_2]_s$ laminates [6]. Also, Fig. 5 is the graph in which Equation 9 is compared with Lagace's experimental results and Tsai's predictions [4]. These comparisons are summarized in

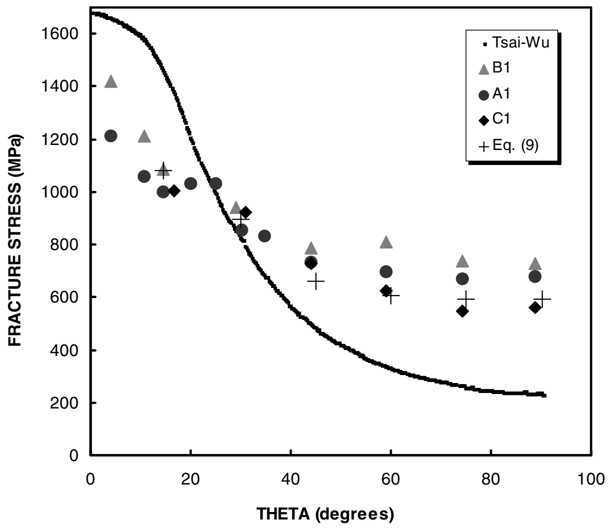

Figure 5 Experimental and predicted unflawed fracture stresses versus lamination angles for the A1, B1, and C1 laminate families.

Table I. The fracture strengths of angle-ply laminates were calculated from the maximum stress criterion.

In Table I, Lagace's results showed differences in fracture strengths with laminate types $[\pm\theta/0]_s$, $[0/\pm\theta]_s$, and $[+\theta/0/-\theta]_s$, though these are the same laminate families. Lagace explained that this is due to the difference in dilamination and the shear stress [4]. Predictions of Equation 9 are same for differing laminate types because in the classical lamination theory, the extensional stiffness matrix, $[A]$, of symmetric laminates is the same for each type. However, the predictions of Equation 9 are in very good agreement with corresponding experimental and theoretical data, as shown in Figs 4 and 5. Therefore, Equation 9 can be applied to predict the fracture strengths of the symmetric laminates.

Fig. 6 shows a side view of the surface-damaged laminate. To predict the fracture strength of surface-damaged laminates, the following assumptions are made:

1. The gradual failure model is applicable.
2. The surface-damaged laminate is symmetric.
3. Young's modulus of unflawed angle-ply laminate ($E_\theta^{(k)}$) is the same as that of flawed laminate ($E_\theta^{(h)}$).

Suppose that a symmetric angle-ply laminate is damaged to mth oriented plies from the surface as shown in Fig. 6. If the damaged layers are considered as new oriented layers, the surface-damaged laminate can be

TABLE I Average fracture strengths for laminate types and calculations (all units in MPa)

Angles	$[\pm\theta/0]_s$ (A1)	$[0/\pm\theta]_s$ (B1)	$[+\theta/0/-\theta]_s$ (C1)	Calculated values
15	998	1003	999	1082
30	855	945	918	896
45	732	787	730	659
60	698	814	585	605
75	672	733	549	593
90	679	732	561	591

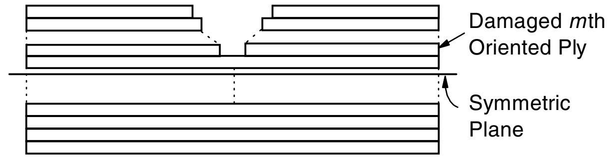

Figure 6 Side view of the surface-damaged laminate (the total n orientations and damaged m orientations).

regarded as a laminate consisting of plies with $n+m$ orientations, and the load–strain curve has the total $n+m-1$ sections. Equation 10 can then be deduced from Equation 9, where σ_0 is the fracture strength of unflawed laminates and σ_N is the fracture strength of flawed laminates.

$$\sigma_{\mathrm{d}} = \frac{1}{T_{\mathrm{total}}}\left[\sum_{k=1}^{n+m-1}\left(K^{(k)}-K^{(k+1)}\right)\varepsilon_k + K^{(n+m)}\varepsilon_{n+m}\right],$$

$$\text{where}\quad K^{(k)} = A_{11}^{(k)} - \frac{A_{12}^{(k)^2}}{A_{22}^{(k)}},$$

$$\varepsilon_k = \frac{\sigma_0}{E_\theta^{(k)}},\quad \varepsilon_h = \frac{\sigma_N}{E_\theta^{(h)}},\quad \text{and}\quad E_\theta^{(k)} = E_\theta^{(h)}. \quad (10)$$

It is crucial to the validity of Equation 10 that σ_0 and σ_N should be first calculated by other criteria or measured experimentally, since the strains at failure of each layer should be calculated. Equation 11 indicates the transformation rule in the surface-damaged laminate.

$$[A]^{(k)} = \sum_{p=k}^{n+m} T_p[Q]_{\theta_p},\quad \text{where}\quad [Q]_{\theta_\alpha}^{\text{nohole}} = [Q]_{\theta_\beta}^{\text{hole}}. \quad (11)$$

We performed experiments to prove Equation 10. A carbon unidirectional prepreg USN 125A (Dupont Inc.) was used with tensile strength 2.2 GPa, Young's modulus 140 GPa, and Poisson's ratio 0.31. The holes were made by a manual punch having diameter 4.4 mm. Five types of laminates consisting of six layers were fabricated: unflawed laminate, and laminates holed at 1 layer, 2 layers, 3 layers, and 6 layers from the surface. The thickness, length, and width of specimens were respectively 0.74, 300, and 25 mm. A UTM (Shimadzu Inc.) was used as a test machine and the fracture loads were measured at a the cross head velocity of 5 mm/min. Fig. 7 is a side view for the laminate holed at three layers with the tensile direction the same as the fiber direction. First, σ_0 and σ_N were measured by experiments with unflawed and six holed laminates. Then, the fracture strengths were calculated from Equation 10 using these data. Fig. 8 shows a comparison of the experimental results with Equation 10. There is very close agreement.

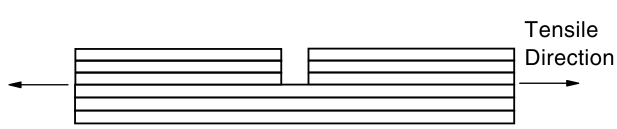

Figure 7 Side view of the fabricated laminate (holed 3 layers).

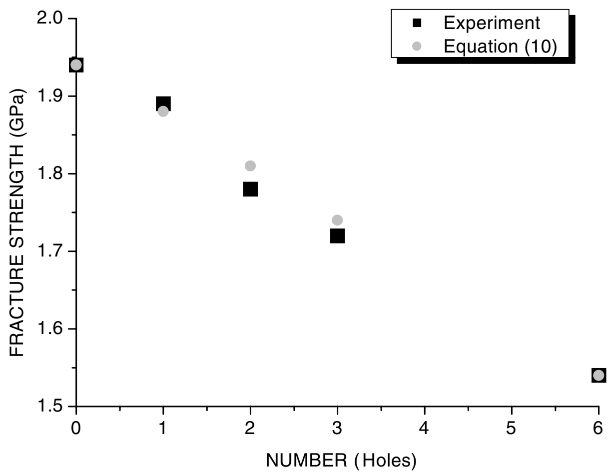

Figure 8 Experimental and predicted fracture strengths versus the number of damaged layers of the fabricated laminate.

In this study, to predict the fracture strength for surface-damaged laminates, Equation 9 for the fracture strength of symmetric laminates is derived by applying the classical lamination theory and the gradual failure model. Equation 10 for the fracture strength of surface-damaged laminates is then derived from Equation 9. To verify these equations, their predictions are compared with Lagace's and Tsia's experimental data. The results show good agreement with previous experiments. These equations can therefore be applied to predict the fracture of surface-damaged composite structures.

Acknowledgment
This work was supported by the Center for Intelligent Surgery System (CISS-02-PJ3-PG6-EV04-0003).

References

1. B. D. AGARWAL and L. J. BROUTMAN, "Analysis and Performance of Fiber Composites" (Wiley-Interscience, 1980) p. 183.
2. R. F. GIBSON, "Principles of Composite Materials Mechanics" (McGraw-Hill, 1994) p. 43.
3. J. M. WHITNEY, "Structural Analysis of Laminated Anisotropic Plates" (Technomic, 1987) p. 1.
4. S. W. TSAI and E. M. WU, *J. Comp. Mater.* **5** (1971) 58.
5. P. A. LAGACE, "Static Tensile Fracture of Graphite/Epoxy" (Doctoral Thesis at MIT, 1982).
6. H. T. HAHN and S. W. TSAI, *J. Comp. Mater.* **7** (1973) p. 102.

Received 27 October
and accepted 30 December 2003